Formation of C_{60} clusters via Langevin molecular dynamics

James R. Chelikowsky
Department of Chemical Engineering and Materials Science, Minnesota Supercomputer Institute, University of Minnesota, Minneapolis, Minnesota 55455
(Received 30 December 1991)

We examine the formation of C_{60} clusters via a Langevin molecular-dynamics simulation. Our simulation incorporates a carbon interatomic potential which reproduces correctly the binding energy and bond lengths of the stable carbon polymorphs. We find that it is possible to nucleate a C_{60} fullerenelike cluster with no symmetry, or volume imposed constraints from a "weakly" interacting "hot gas" of carbon atoms. We propose that the growth sequence for C_{60} fullerene in the initial phase is dominated by the nucleation of long carbon chains. As the nucleation process proceeds, these chains branch and form polycyclic rings. We find an abrupt onset of ring formation at a temperature which corresponds approximately to the melting point of graphite. Also, we propose an annealing technique that expedites the formation of stable clusters.

I. INTRODUCTION

Understanding the nucleation process by which the C_{60} fullerene molecule forms is a formidable undertaking.[1-5] The molecule has complete symmetry since each of its 60 carbon atoms resides in an identical environment. It is hard to envision a process for the formation of such a highly symmetric molecular system of this size. Crystal growth can be envisioned to proceed from a small nucleating "seed" and ending in an interface, or free surface. In this manner, an ideal, periodic structure can be formed with the surface, or interface, being an inherent "defect." For C_{60}, no such interfacial "defect" is present, and the nature of a nucleation seed is problematic. Most models for the creation of C_{60} fullerenes (Refs. 4 and 5) avoid details of the process. Some workers have speculated that the formation of C_{60} proceeds via a nucleation seed of a symmetric "subunit" such as a pentagonal, or hexagonal ring, or combinations thereof. Typically, the hydrocarbon corannulene molecule which contains a fivefold carbon ring surrounded by sixfold rings serves as a generic example of a nucleation site.[4] This molecule is thought to be nonplanar and effectively forms half of the base of a C_{60} molecule. However, this picture excludes any discussion of how the nucleation site is formed, and relies on thermodynamic arguments to justify the C_{60} fullerene structure. While such arguments are valid in terms of "ground-state" stability, they do not illuminate the details of the kinetics.

A different point of view can be considered. Suppose one starts from a gas of "weakly interacting" carbon atoms. One can ask such questions as: "What are the most stable units of carbon at high temperatures?" and "How do these units change as the system is cooled?" In our approach, we will study carbon atoms in a hot gas and examine the evaluation of chains, rings, and fullerenes as the system is cooled. By examining this environment, we hope to learn likely "seeds" from which the C_{60} molecule may grow, and determine the qualitative features which may enter the formation process.

To understand dynamical processes, we have developed an interatomic potential for carbon which will allow complex systems to be simulated. For systems of more than a dozen atoms, it is not possible to model the dynamics of a system via direct quantum-mechanical calculations, except for extraordinarily short time spans. A common practice[6-9] is to replace quantum-mechanical interactions by "classical interactions" which are derived from interatomic potentials. The implementation of "classical" interatomic potentials can reduce by orders of magnitude the computational effort for dynamical simulations. This reduction in computational effort gains little if the essential features of the system are lost in the transcription of quantum-mechanical interactions into classical forces. Clearly, this transcription can be made for closed-shell systems. The use of van der Waals potentials for simulating the inert gases is a common example. Also, for ionic materials, Born-Mayer potentials work very well.

For solids composed of open-shelled species, the issue of generating accurate potentials is unresolved. For group-IV-element solids, the diamond structure is a signature of quantum-mechanical covalent bonding forces. Open structures cannot be rationalized by consideration of two-body, or classical, forces. However, the construction and implementation of three-body, or angular, forces for these systems is nontrivial. Some workers have suggested that such potentials are of limited utility at best as *many-body* interactions, by definition, are strongly dependent on the local environment. We have found that this need not be the case, if some care is taken in choosing the data base to construct interatomic potentials. For silicon,[8] we used two divergent data sets: (a) the high-pressure phases of silicon which contain "overcoordinated" silicon atoms, i.e., atoms with more than four bonds, and (b) clusters of silicon which contain "undercoordinated" species. Our goal was to build these divergent bonding configurations into our potential. We succeeded in

this attempt as much as we could predict "magic" numbers for the reactivity of small silicon clusters and, more recently, to predict an isomeric transformation of silicon clusters.[8,10]

Here we focus on building a potential for carbon which will be applicable to modeling the nucleation of the C_{60} molecule. Unlike silicon, carbon can exist with multiple-bond formation, and as a consequent, is more challenging. Our starting point will be to consider our silicon potential[8] and make changes to reflect differences between silicon and carbon. Our approach will allow us to examine differences between the two species, and provide a "unified" approach.

With our interatomic potential, we will examine the state of carbon atoms at high temperatures, and the nucleation process, as we quench the system. Our simulation will be focused on Langevin molecular dynamics. This type of simulation allows much longer time steps than traditional molecular dynamics,[11] and allows one to incorporate a "heat bath" to control the cluster temperature in a physically appealing manner.

II. INTERATOMIC POTENTIALS FOR CARBON

To construct an interatomic potential for carbon, we use a functional form which is similar to that of our silicon potential. To fit the parameters of this potential, we employ the structural energy of various other polytypes of carbon, e.g., carbon in the body-centered-cubic, simple-cubic, and face-centered-cubic structures, as obtained from *ab initio* pseudopotential total-energy calculations.[12,13] Pseudopotential calculations have yielded accurate structural properties for known forms of carbon, and should be accurate for hypothetical dense phases.[12]

The form of our bulk carbon potential, following the silicon work, is given by

$$E[\{\mathbf{R}\}]=\sum_{\substack{i,j\\(i<j)}}[A\exp(-\beta_1 R_{ij}^2)/R_{ij}^2 - g_{ij}\exp(-\beta_2 R_{ij}^2)/R_{ij}] \ . \quad (1)$$

R_{ij} is the interatomic distance between (i,j) and the many-body interactions are contained within the factor g_{ij}. g_{ij} is constructed to be large for covalent, open-structure systems (structures with large bond angles, such as diamond or graphite) as compared to close-packed systems such as the face-centered-cubic structure. We define g_{ij} as

$$g_{ij}=g_0+g_1 S_{ij}S_{ji} \ , \quad (2)$$

where

$$S_{ij}=1+\langle\cos(3\theta_{ijk})\rangle \ ,$$

$$\langle f(\theta_{ijk})\rangle=[f]/[1] \ ,$$

$$[f(\theta_{ijk})]=\sum_{\substack{k\\k\neq i,j}} f(\theta_{ijk})\exp(-\lambda_1\theta_{ijk}^4)\exp(-\lambda_2 R_{ijk}^4) \ ,$$

with $R_{ijk}=(R_{ij}+R_{ik})/2$. θ_{ijk} is the angle between $\mathbf{R}_{ij}$ and $\mathbf{R}_{ik}$. This form represents a short-ranged function which has sharp angular and radial cutoffs. The factor S_{ij} ranges from 0 for metallic structures with small bond angles to 2 for covalent systems. Also, for $\theta_{ijk}<\pi/3$ $(\theta_{ijk}>2\pi/3)$ we saturate $\cos(3\theta_{ijk})$ so that $\cos(3\theta_{ijk})=-1$ $[\cos(3\theta_{ijk})=+1]$.

From a rescaling of our silicon potential, we find the denser polytypes of carbon are poorly replicated. The energy separation of these dense phases from the diamond structure is too small, e.g., the separation between the simple cubic structure and diamond is nearly 1 eV, instead of the ~3-eV separation determined by pseudopotential calculations.[12] This error is to be expected as the angular energy terms in silicon are less important than in carbon, i.e., bond-bending forces in carbon phases are stronger than in the corresponding silicon phases. Upon refitting the angular terms, we could move these polytypes to higher energies. Also, a refitting is necessary to stabilize graphite versus the diamond structure: by penalizing structures with small bond angles, the diamond structure becomes slightly less energetically favorable than graphite. Our potential yields accurate energies and bond lengths for carbon in the diamond and graphite structures and does a reasonable job for the denser polymorphs of carbon. In Fig. 1 we compare the equations

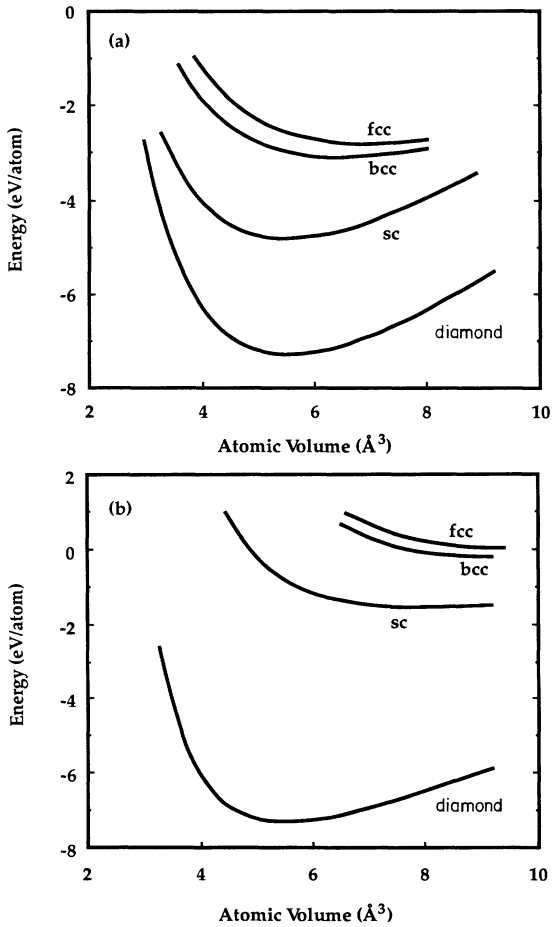

FIG. 1. Equations of state for carbon in the diamond (diamond), simple-cubic (sc), body-centered-cubic (bcc), and face-centered-cubic (fcc) structures as calculated from (a) *ab initio* pseudopotentials (after Ref. 12) and (b) interatomic potentials as defined in the text.

of state from our interatomic potentials to *ab initio* pseudopotential calculations for diamond and the denser phases.[12] In Table I we compare the structural properties of diamond and graphite as determined by our interatomic potential to experiment. Values for the potential parameters are $A=45.59$ eV Å^2, $\beta_1=0.80$ Å^{-2}, $\beta_2=0.35$ Å^{-2}, $g_0=1.33$ eV Å, $g_1=6.09$ eV Å, $\lambda_1=(2/\pi)^4$, and $\lambda_2=0.961$ Å^{-4}.

We note that graphite is a major challenge for any carbon interatomic potential. The forces within the graphitic plane are covalent whereas the interplanar forces are commonly attributed to van der Waals interactions. The form of our potential does not contain van der Waals interactions, and so one might expect some significant shortcomings. Schabel and Martins[14] have suggested the cohesive energy of graphite as a function of the interlayer distance, given by the c-axis structural parameter, can be written as a Morse potential of the form

$$E(c)=E(c_0)+b_1\{\exp[-b_2(c-c_0)]-1\}^2 , \quad (3)$$

where c_0 corresponds to the equilibrium c parameter, b_1 corresponds to the interplanar binding energy, and b_2 is a parameter giving the range of the interplanar interactions. In Table I we give values to the fit of our potential to this functional form. In Fig. 2 we show the quality of this fit and compare our interatomic potential calculation to the pseudopotential calculation. As expected, we do not replicate the interplanar binding energy. Our potential yields a binding energy of approximately 0.5 eV/atom whereas experiment and the pseudopotential work suggests a much smaller binding energy of approximately 0.02 eV/atom. Our large binding energy is reflected in the uniaxial compressibility of graphite which is about a factor of 3 smaller than experiment. Unlike the quantum calculations which have many electronic degrees of freedom, our potential has only "nuclear" coordinates. A common occurrence in this situation is for the energy differences between structures to be exaggerated.[8] Despite this expected deficiency, our "predicted" value for the c axis is 6.2 Å, in credible agreement with the experimental value of 6.7 Å. Also, the functional form of the crystal energy versus the c parameter is reproduced accurately with a Morse potential. The range of our po-

TABLE I. Structural properties of carbon in the diamond, graphite, and C_{60} fullerene forms from experiment and theory. The theoretical values are determined from the interatomic potential as defined by Eqs. (1) and (2) and (4)–(6).

Structure	Experiment	Theory
Diamond		
Cohesive energy	7.37 eV/atom[a]	7.28 eV/atom
Lattice constant	3.57 Å[b]	3.53 Å
Bulk modulus	4.42 Mbar[c]	4.7 Mbar
Pressure derivative of bulk modulus	~4[d]	5.3
Graphite		
Cohesive energy	7.41 eV/atom[e]	7.33 eV/atom
Lattice parameters:		
a_0	2.45 Å[f]	2.51 Å
c_0	6.67 Å	6.17 Å
Morse parameters:		
b_1	22.8 meV/atom[g]	580 meV/atom
b_2	0.971 Å^{-1}	0.783 Å^{-1}
Uniaxial compressibility	2.7×10^{-12} cm^2/dyne[h]	0.7×10^{-12} cm^2/dyne
C_{60}		
Cohesive energy	~7.0 eV/atom[i]	6.9 eV/atom
Bond lengths:		
Short bond	1.40 Å[j]	1.42 Å
Long bond	1.47 Å	1.49 Å

[a]L. Brewer (unpublished).
[b]J. Donohue, *The Structure of the Elements* (Wiley, New York, 1974).
[c]H. J. McSkimin and P. Andreatch, Jr., J. Appl. Phys. **43**, 9856 (1972).
[d]Estimate from K. Gschneidner, Jr., *Solid State Physics*, edited by H. Ehrenreich, F. Seitz, and D. Turnbull (Academic, New York, 1964), Vol. 16, p. 275.
[e]N. N. Greenwood and A. Earnshaw, *Chemistry of the Elements* (Pergamon, Oxford, 1984).
[f]Y. Baskin and L. Mayer, Phys. Rev. **100**, 544 (1955).
[g]H. Drickamer, Science **156**, 1183 (1967).
[h]R. Nicklow, W. Wakabayashi, and H. G. Smith, Phys. Rev. B **5**, 4951 (1972).
[i]Estimate from pseudopotential calculations, N. Troullier and J. L. Martins (unpublished).
[j]W. Krätschmer, L. D. Lamb, K. Fostiropoulos, and D. R. Huffman, Nature **347**, 354 (1990).

tential shown by b_2 is entirely consistent with the pseudopotential calculations[14] and Thomas-Fermi models[15] which yield $b_2 = 0.8$ Å^{-1}.

If one compares the energy and structure of the C_{60} molecule as determined from experiment[16] and from pseudopotential calculations[17,18] to interatomic potential calculations using the potential defined above, the agreement is not satisfactory. The energy of C_{60} is underestimated by $\sim 20\%$ and, more significantly, the structure is not dynamically stable as compared to a large diamond-structure "fragment." Our interatomic potential as defined above contains no information on isolated carbon rings, or graphitic sheets, as will be important for modeling C_{60}. This situation is similar to silicon. Small silicon clusters are known from sophisticated quantum calculations[19–21] to be close packed in contrast to the ground-state structure of silicon, i.e., the diamond structure. For silicon, it was necessary to change the silicon "bulk" interactions[8] as these interactions would yield "incorrect" cluster structures corresponding to open structure, diamondlike, fragments. We modified the silicon potential so that two-body interactions were strengthened at the expense of three-body interactions. Physically, this change corresponds to strengthening the backbonds of an undercoordinated silicon atom. For carbon, we proceed in a similar manner as we modify the bulk interactions. However, unlike silicon, small carbon clusters are thought to form as chains, or rings, and not as close-packed fragments.[22] One can view this difference as arising from multiple-bond formation in carbon which is absent, or nearly so, in silicon. We are primarily interested in replicating the behavior of isolated sheets of graphite. We do not expect to be able to model small carbon clusters in which double or triple bonds might exist besides single bonds.

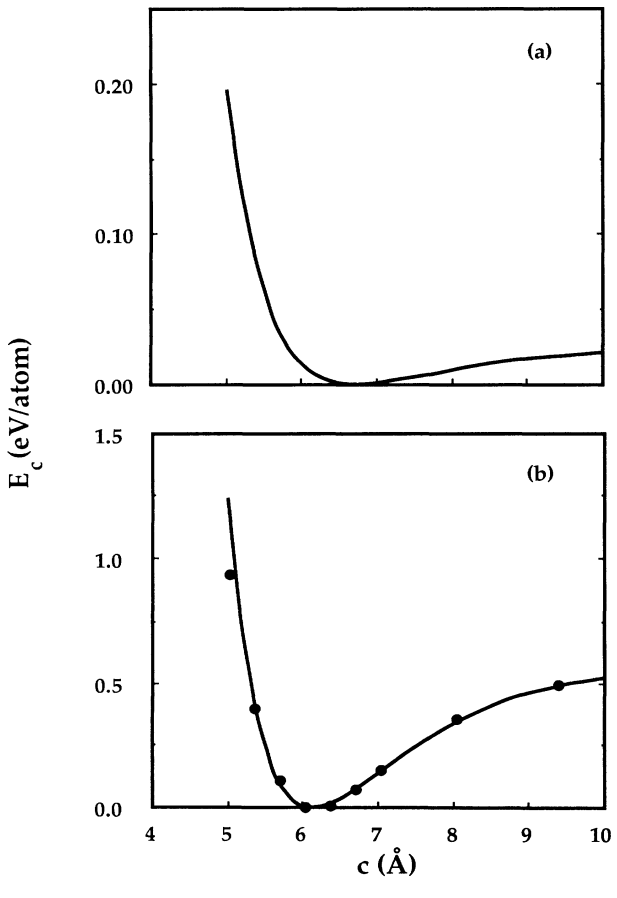

FIG. 2. Total energy of graphite plotted vs the c-axis parameter. Two calculations are shown: (a) is from *ab initio* pseudopotential calculations (after Ref. 14) and (b) interatomic potentials as defined in the text. The solid curves are determined by a fit to a Morse potential [Eq. (3) in the text]. The energy zero is taken to be the equilibrium energy of graphite. Note the change in scale.

We alter bulk interactions to strengthen the bonds in C_{60}. Also, we include an additional angular factor which ensures that isolated graphitic sheets will not be stable in a planar geometry, but will prefer to "buckle." The form of this modification follows from our silicon work,[8] and is fixed by a comparison to total-energy calculations[17,18] for the solid-state C_{60}.[16]

We introduce a "dangling-bond vector" $\mathbf{D}_i$. This vector is defined as

$$\mathbf{D}_i = -\sum_{j,j\neq i} \mathbf{R}_{ij} \exp(-\lambda_3 R_{ij}^2) \Big/ \sum_{j,j\neq i} \exp(-\lambda_3 R_{ij}^2) \ . \quad (4)$$

This vector vanishes for the crystalline polymorphs, but will be present for systems which do not have a local inversion center such as the C_{60} molecule. We define an angular term as

$$Q_{ij} = 1 + z D_i \sin[\alpha(\theta_{ij} - \pi/3)] \ . \quad (5)$$

We combine this term with the dangling bond to modify our g_{ij} term. We take

$$\Delta g_0 / g_0 = \mu(Q_{ij} Q_{ji} - 1) \exp(-\beta_2 R_{ij}^2) \ . \quad (6)$$

The C_{60} bonds will now be stabilized versus diamond fragments, and the angular term will facilitate "buckling" of graphitic sheets. We note two features of this potential which differ from silicon.[8] The range of the bond-strengthening term is longer than silicon, i.e., we implement a Gaussian weighting in Eq. (4) instead of a $\exp(-\lambda_3 R_{ij}^4)$ term. The range of this term must exceed the size of one hexagonal ring to ensure that ordering between fivefold and sixfold rings is possible. We do not weaken the bulk *angular* terms in Eq. (6), i.e., change g_1, as we did for silicon. For silicon clusters, this modification led to close-packed clusters which would not be correct for carbon. The potential parameters for Eqs. (4)–(6) are $\alpha = 2.25$, $z = 0.132/$Å, $\lambda_3 = 0.0319$ Å^{-2}, and $\mu = 4.0$.

Our interatomic carbon potential from Eq. (1) and (2), as modified in Eqs. (4)–(6), yields a dynamically stable C_{60} fullerene. The bond lengths and energy are given in Table I, and are compared to theoretical estimates for the cohesive energy of the molecule and to experimental values for the bond lengths. Two bond lengths exist for C_{60}. The longer bond is shared between fivefold and sixfold rings; the shorter bond is shared between sixfold rings, respectively. The bond lengths in Table I are taken

from the molecular solid; we do not expect the bond lengths to be significantly different for the molecule.

III. LANGEVIN SIMULATIONS OF THE FORMATION OF C_{60} CLUSTERS

Assuming our interatomic potential replicates accurately the forces between interacting carbon atoms, we need a procedure for determining the optimal structure for a given number of atoms. We will integrate the equation of motion of a particle using the *Langevin* or, *Brownian,* molecular-dynamics approach.[11] Within this approach, a particle is considered to move in a viscous medium and experiences a rapidly fluctuating random force besides the interatomic forces from other particles. The fluctuations of the random force are dictated by the temperature of the medium.

This method has several advantages over other simulation techniques. The time steps used to integrate the resulting equations of motion[11] can be quite long, e.g., one or two orders of magnitude longer than other molecular-dynamical simulations. This will permit longer time frames to be considered. The temperature of the system is introduced in a natural way without having to scale the kinetic energy of the system in an *ad hoc* fashion. The thermal bath has a physical analogy to the real system: Namely, the C_{60} molecule is nucleated in a buffer-gas environment.[2,3] The viscous medium can play the role of the buffer gas. The only "significant" disadvantage of this method is shared with other simulation methods, e.g., the time frame of a molecular-dynamics simulation is much shorter than relevant experimental times.

The trajectory of a free particle within this picture[11] is given by

$$m\frac{d\mathbf{v}}{dt}=-\gamma\mathbf{v}+\mathbf{G}(t,T)\ , \tag{7}$$

where m is the mass of a carbon atom, γ is the viscosity, and $\mathbf{G}$ is a rapidly fluctuating force which is temperature dependent. This equation can be used to describe a particle in a hypothetical viscous medium executing Brownian motion if the random forces have a zero mean, and a correlation function for each ith-spatial component given by

$$\langle G_i(t)G_i(t')\rangle=2\gamma k_B T\delta(t-t')\ . \tag{8}$$

The viscosity parameter ensures one that the fluctuation-dissipation theorem is obeyed, i.e., the work done by the random force is dissipated by the viscous friction.[11,23] The stochastic nature of this simulation will destroy information about the initial condition of the system and drive the system to equilibrium which is characterized by the temperature.

When we consider an additional force which arises from particle-particle interactions, we have the coupled dynamical equations

$$\begin{aligned}\frac{d\mathbf{r}}{dt}&=\mathbf{v}\ ,\\ m\frac{d\mathbf{v}}{dt}&=\mathbf{F}-\gamma\mathbf{v}+\mathbf{G}(t,T)\ .\end{aligned} \tag{9}$$

Owing to the random thermal fluctuations in $\mathbf{G}$, the particles explore many difference configurations at high temperatures. We then cool the system by lowering the thermal fluctuations in the random force $\mathbf{G}$. If we cool slowly enough, we hope to "quench" out the *lowest energy* structure for particles interacting with the given interatomic potentials.

To simulate the nucleation of C_{60} fullerenes, we consider an initial configuration consisting of a "large" box of 60 carbon atoms. These atoms are not allowed to interact significantly. Specifically, we consider a cube of 12 Å on a side and deposit the atoms randomly within this box. We impose one constraint: the atoms are not allowed to be within 2 Å of one another. This allows us to contain the 60 atoms, yet not have them overly "biased" by the initial configuration.[8] We chose an initial temperature for the atoms in this to be 7000 K. This temperature is chosen to be well above the melting point of solid carbon. Our initial condition corresponds to a "hot, chaotic gas" of weakly interacting carbon atoms. The viscosity parameter was taken to be $\gamma=0.001$ in atomic units.

Within the Langevin molecular-dynamics simulation, we quench this system and observe the nucleation process. There are two goals to our simulation. First, we wish to observe what sort of structures form as we rapidly cool this system. Second, we will modify this simulation process in an attempt to nucleate the lowest-energy structure possible. With respect to the first goal, we quench the system as with our silicon cluster work. The time step for the integration of motion is 2 fsec with a total simulation time of 20 psec. During this time, the box temperature is reduced from 7000 to 1000 K.

Initially, short chains are formed as illustrated in Fig. 3(a). At sufficiently high temperatures, it seems clear that entropic considerations will dominate the structural properties of the "hot gas." For a given number of atoms, a chain will be favored by entropy over a ring. Thus, it is not surprising that chains are formed first. This is consistent with earlier work[24] which suggested that chains would be stable at high temperatures. It is surprising that these chains grow to fairly long units, e.g., over ten atoms in length. However, our carbon potential, and presumably the "real" carbon interactions favor large angles in the chain growth which inhibits ring closure [Fig. 3(b)] for small carbon chains. At moderately high temperatures ($\sim$5000 K) enthalpic considerations begin to influence the quench, and the chain structure begins to change. The chains form branches and eventually hexagonal ring configurations start to appear near 4000 K [Fig. 3(c)]. This suggests that one may not be able to nucleate C_{60} fullerenes above this temperature. It also suggests that the solid state, i.e., graphite, may not be nucleated above this temperature. This finding is consistent with estimates of $\sim$4000–5000 K for the melting point of carbon.[25] The ring structure is maintained to lower temperatures [Fig. 3(d)].

One issue of some interest is the evolution of rings as the temperature is lowered. It has been speculated that fivefold ring formation is crucial to the buckling of graphitic sheets. This speculation is strongly supported by

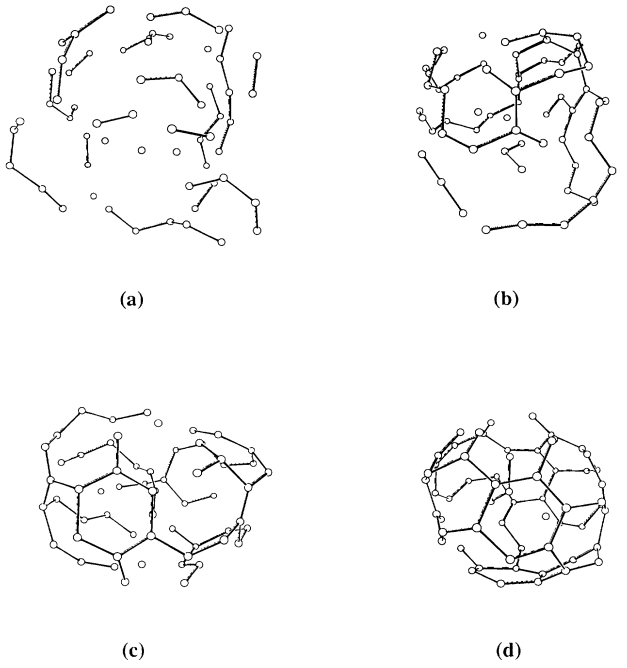

FIG. 3. Structures illustrating the nucleation process for a cluster of 60 carbon atoms. (a) The cluster is at 6000 K. Short chains appear. (b) The cluster is at 5000 K. Longer chains are formed which start to branch. (c) Hexagonal rings begin to form at 4000 K. (d) A spheroidal cluster is formed with sixfold rings formed (2000 K).

thermodynamic arguments.[5] Perfect sheets of graphite have dangling bonds at the edge of the sheet. By buckling the sheets, the number of dangling bonds is reduced per unit area. If the sheet closes on itself to form a sphere such as C_{60}, then the dangling bonds are removed altogether. To examine the evolution of the ring structure in more detail, we determined the percentage of atoms of the system which reside in rings. Owing to the stochastic nature of the hot gas, it is not trivial to decide when a ring structure exists. We used a simple criterion: namely, when two atoms are within 20% of the ideal bond length of the diamond crystal, then a bond is said to exist between the atoms. By using a large bond-length criterion, we reduce unphysical fluctuations of the bond number.

We examined both fivefold and sixfold ring formation and found that fivefold rings are less common than sixfold rings over the entire temperature range. This is not surprising as fivefold rings are energetically less favorable with our potential than are sixfold rings. In Fig. 4, we show the evolution of sixfold rings as a function of temperature. Fivefold ring evolution follows a similar behavior. We indicate the average binding energy, i.e., the potential energy of the system, as a function of the quench temperature. At high temperatures, few atoms exist in rings. As the temperature is lowered a strong onset of ring nucleation occurs near ~4800 K. This "first-order" change is replicated in the binding energy, and is consistent with the melting point of graphite.

Although our anneal is not sufficiently slow to produce a highly symmetric structure, the lowest temperature structure in the anneal corresponds to a spheroidal cluster with many-linked hexagonal rings. This is true for the runs we have examined, and appears not to be a strong function of the quench rate, at least for quick quenches. However, the energy of this structure is somewhat removed from the energy of an ideal C_{60} molecule. The energy we calculate for this structure is ~6.7 eV/atom as contrasted with the energy of the ideal C_{60} (Ref. 18) of ~7.0 eV/atom. Because our quench is quick, we often find atoms trapped in the interior of the spheroid cluster. These atoms are in energetically unfavorable sites because of the rapid kinetics.

Our second goal is to search for the global minimum structure, i.e., the ground-state structure. Such a search is notably certain to fail from the start. For any system of modest size, e.g., over 20 atoms, finding the phase space occupied by the ground-state structure is usually beyond our computational capability using standard techniques, e.g., molecular dynamics and simulated annealing. For a highly symmetric structure as the C_{60} molecule, the possibility of a successful search is even more remote. We seek a more limited objective. Namely, we hope to find a low-energy structure which resembles the C_{60} molecule.

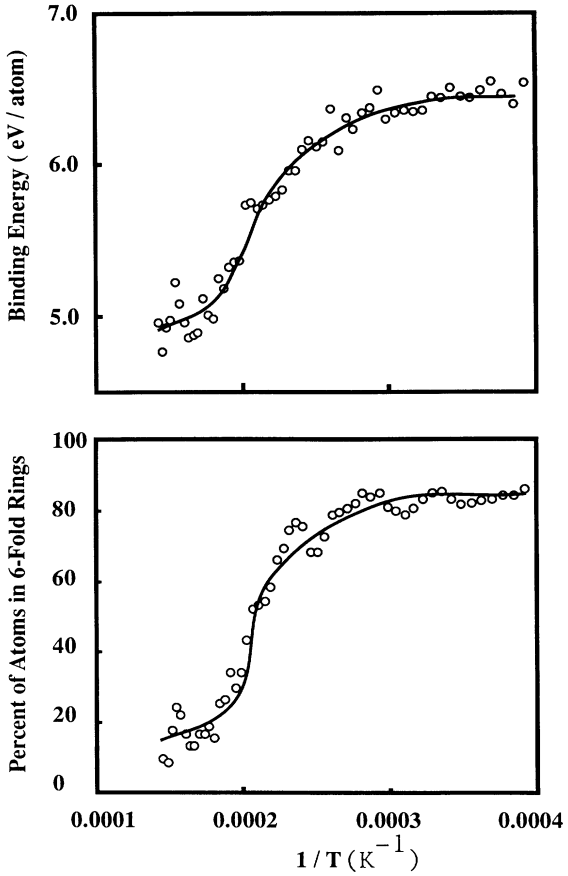

FIG. 4. Binding energy per atom (top) and the percent of atoms in sixfold rings (bottom) as a function of the quenching temperature. The binding energy does not include kinetic energy. Note the abrupt onset of ring formation below ~5000 K.

We tried the following algorithm. We take our quenched structure in Fig. 3(d) and prepare a new starting configuration for further annealing. To prepare the new starting configuration, we remove all the energetically unfavorable atoms from the cluster. We define "unfavorable" to include atoms whose binding energy is more than one standard deviation removed from the average binding energy in the cluster. For a structure such as the one in Fig. 3(d), about 10–15 atoms are involved. These energetically unfavorable atoms are then randomly placed within the annealing cube with two constraints. The new position of these atoms cannot be within 2 Å of an existing atom, nor can they be placed within 2 Å of an original site which was found to be unfavorable. These constraints ensure that the prepared structure is topologically distinct from the previous one. We then repeat the annealing process, i.e., we take an initial temperature of 7000 K and rapidly quench to 1000 K. By repeating this process, we could find a lower-energy structure which contained no atoms within the interior of the cluster. Our optimal cluster was annealed for a longer period, i.e., approximately 100 psec, from 6000 to 300 K.

An advantage of interatomic potentials is that one can examine the binding energy for individual atoms. The distribution of binding energies for various stages of our annealing procedure is shown in Fig. 5. In the initial configuration of atoms we have an energetic distribution which is centered near zero binding energy [Fig. 5(a)]. There is some spread to this distribution as the atoms are allowed to interact weakly. After a quick quench the average binding energy is increased, but there is a large spread of the atomic energies as the quench is so rapid as to trap atoms in unfavorable bonding configurations. For example, the atoms in the interior of the spheroid shown in Fig. 3(d) have a binding energy which is less than half that of the most favorable bond configuration. After a reanneal, we find that the distribution becomes sharper as the system has fewer defects. However, we found that we could not further sharpen the distribution by continuing to repeat the process. One issue involves the rate at which we reanneal. It may be that unless we cool far more slowly than the current ~ 100 psec interval, we cannot anneal out defects which remain in the final structure. The procedure of quenching, heating the system, and reannealing has an analogy to experiment where one can heat the buffer gas and/or apply a laser beam to the system to reheat the clusters.

The lowest energy structure we found is displayed in Fig. 6. The energy of this structure is comparable to that of the ideal C_{60} to within ~ 0.05 eV/atom. The structure contains no interior atoms and is dominated by sixfold and fivefold rings. We are successful with this algorithm in producing a C_{60} fullerenelike structure.

Two prominent defects occur in our "best" structure when compared to the ideal C_{60} structure. First, pentagonal rings often share a common base. The bond length corresponding to the shared base is $\sim 10\%$ longer than the other bond lengths of the pentagon. The shared pentagons may also be considered to form an eight-membered ring with a weak bridging bond. This configuration may be seen in the top part of Fig. 6. Another common defect is for two fivefold rings to share a common base, and have the length of the shared base increased so that an atom bridges the base forming two "puckered" sixfold rings. Both defects suggest a strong interplay of the bond strengths between atoms in fivefold and sixfold rings. We note that such defects have been suggested on the basis of a semiempirical tight-binding simulation.[26] In this simulation, a C_{60} fullerenelike structure was obtained when the atoms were constrained to reside in a spherical cavity and a high pressure (~ 0.5 Mbar) applied to the system. We have not found it necessary to invoke such a constraint. However, we should note that our rapid quench and the initial configuration which localizes the atoms to a box may mimic the pres-

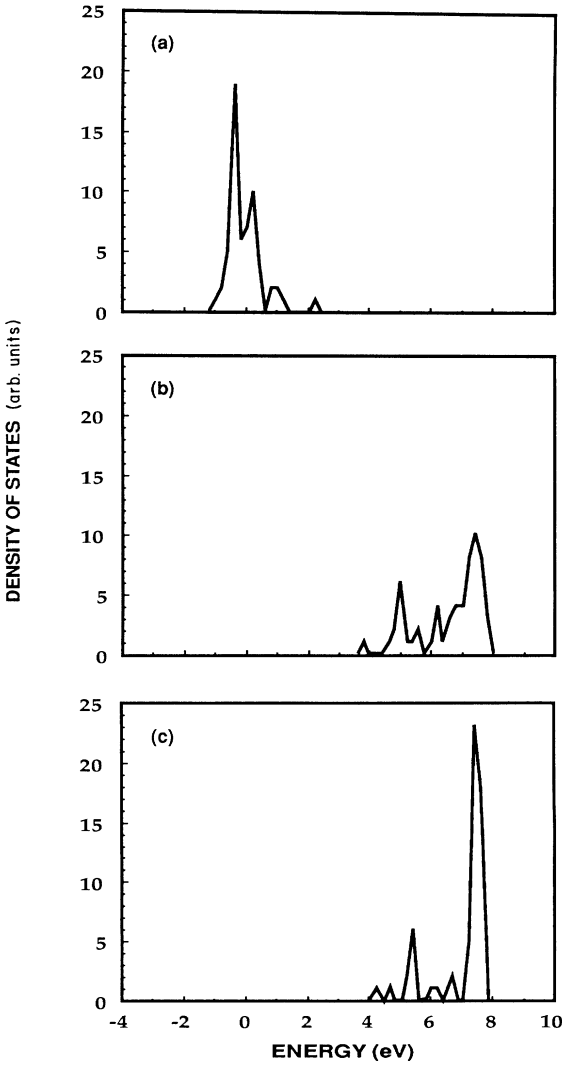

FIG. 5. Density of states (in arbitrary units) for carbon atoms as a function of the binding energy per individual atoms. (a) Density of states for the initial configuration. The energy zero is taken to be for an isolated carbon atom. (b) Density of states after a quick quench. (c) Density of states after reanneal of the cluster as explained in the text.

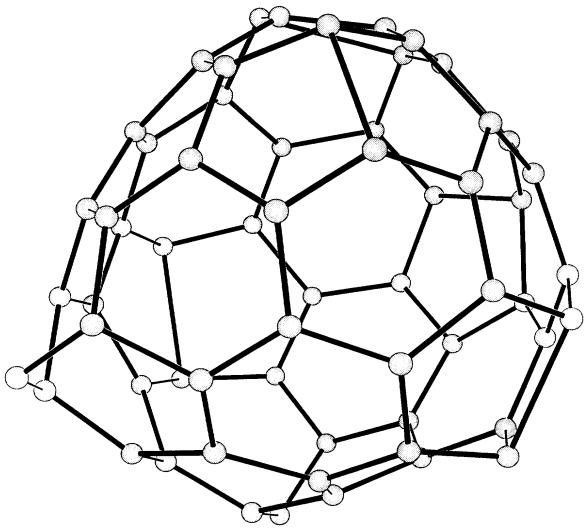

FIG. 6. Lowest energy structure formed from the annealing simulation. Note the presence of both fivefold and sixfold rings. This structure contains elements in common with C_{60}; however, defects still dominate the structure.

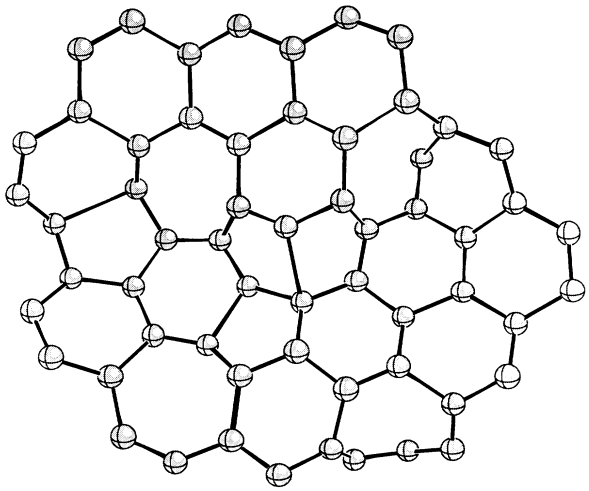

FIG. 7. Structure of carbon atoms quenched within a quasi-two-dimensional constraint. The structure resembles a graphitic sheet with a number of defects introduced by the quick quench.

sure constraint to some extent.

We note that recent estimates from quantum chemistry[27] have been made for the energy of placing two fivefold rings next to one another. The energy of this defect is fairly high $\sim 1-2$ eV as the defect introduces significant strain into the C_{60} molecule.[28] The mechanism by which this defect is created and how it may be destroyed is one of the major puzzles of the formation of C_{60}. It may be that our anneal is simply too rapid. Another possibility is that our first study is unrealistic as we constrained our system to 60 atoms. A monomer, dimer, or trimer reservoir may be necessary for the growth of a perfect C_{60} molecule. Such a suggestion is consistent with the fact that no natural means of growing C_{60} exists: C_{60} appears only when the carbon vapor is accompanied in a helium buffer-gas environment under the "right" temperatures and pressures.

We note that it is possible to check our potential by growing two-dimensional forms of carbon. We have constrained our system to a "quasi"-two-dimensional system by placing the atoms in a box whose dimensions were fixed to $12 \times 12 \times 2$ Å. Using the same anneal procedures as for C_{60}, we could grow a "graphitic like sheet." The binding energy of this sheet was ~ 0.5 eV/atom less than the C_{60} fullerenelike structure we formed in three dimensions. The chief reason for the lower binding energy is the existence of low coordinated atoms at the edge of the graphite sheet. Like our structure in Fig. 6, which contains many defects when compared to the ideal C_{60}, the "graphite" grown in our simulation (Fig. 7) possesses a number of defects owing to the rapid growth process.

IV. CONCLUSIONS

We have examined the nucleation of C_{60} fullerenes by a Langevin molecular-dynamics simulation. Our simulation incorporates a carbon interatomic potential which correctly reproduces the diamond and graphitic forms of carbon in terms of bond energies and bond lengths. The potential also reproduces the energy of C_{60} and the bond lengths. Our simulation considers the nucleation of C_{60} from a hot gas of weakly interacting carbon atoms. We find in the initial stages of the simulation at high temperatures, carbon-chain structures form. As the system is cooled, the chains become branched and form polycylic rings. At sufficiently long anneals, the cluster formed resembles the C_{60} molecule with defects. The defects consist primarily of shared fivefold rings and puckered sixfold rings. We have also been able to simulate the growth of a graphite sheet and find that similar defects occur.

ACKNOWLEDGMENTS

Acknowledgment is made to the Donors of the Petroleum Research Fund, administrated by the American Chemical Society, for partial support of this research. Also, we would like to acknowledge partial support for this work by the U.S. Department of Energy of the Office of Basic Energy Sciences (Division of Materials Research) under Grant No. DE-FG02-89ER45391. We would like to acknowledge computational support from the Minnesota Supercomputer Institute and helpful conversations with Dr. J. C. Phillips, Professor R. E. Smalley, and Professor J. L. Martins.

[1]H. W. Kroto, J. R. Heath, S. C. O'Brien, R. F. Curl, and R. E. Smalley, Nature **318**, 162 (1985).
[2]Q. L. Zhang, S. C. O'Brien, J. R. Heath, Y. Liu, R. F. Curl, H. W. Kroto, and R. E. Smalley, J. Phys. Chem. **90**, 525 (1986).
[3]R. F. Curl and R. E. Smalley, Science **242**, 1018 (1988).
[4]H. W. Kroto and K. McKay, Nature **331**, 328 (1988); H. W. Kroto, Pure Appl. Chem. **62**, 407 (1990).
[5]R. E. Haufler, Y. Chai, L. P. F. Chibante, J. Conceicao, C. Jin, L. S. Wang, S. Maruyama, and R. E. Smalley, in *Clusters and Cluster-Assembles Materials,* edited by R. S. Averback, J. Bernhole, and D. L. Nelson, MRS Symposia Proceedings No. 206 (Materials Research Society, Pittsburgh, 1990).
[6]D. W. Brenner, Phys. Rev. B **42**, 9458 (1990), and references therein.
[7]J. Tersoff, Phys. Rev. Lett. **61**, 2879 (1988), and references therein.
[8]J. R. Chelikowsky and J. C. Phillips, Phys. Rev. B **41**, 5735 (1990); **44**, 1538 (1991).
[9]A preliminary version of this work appears in J. R. Chelikowsky, Phys. Rev. Lett. **67**, 2970 (1991).
[10]M. Jarrold and V. A. Constant, Phys. Rev. Lett. **67**, 2994 (1991).
[11]R. Biswas and D. R. Hamann, Phys. Rev. B **34**, 895 (1986).
[12]S. Fahy and S. G. Louie, Phys. Rev. B **36**, 3373 (1987).
[13]J. R. Chelikowsky and S. G. Louie, Phys. Rev. B **39**, 3470 (1984).
[14]M. C. Schabel and J. L. Martins, Phys. Rev. B **43**, 11 873 (1991).
[15]D. P. DiVincenzo, E. J. Mele, and N. A. W. Holzwarth, Phys. Rev. B **27**, 2458 (1983).
[16]W. Krätschmer, L. D. Lamb, K. Fostiropoulos, and D. R. Huffman, Nature **347**, 354 (1990).
[17]J. H. Weaver, J. L. Martins, T. Komeda, Y. Chen, T. R. Ohno, G. H. Kroll, and N. Troullier, Phys. Rev. Lett. **66**, 1742 (1991); M. B. Jost, D. M. Poirier, N. Troullier, J. L. Martins, J. H. Weaver, R. E. Haufler, L. P. F. Chibante, and R. E. Smalley, Phys. Rev. B **44**, 489 (1991).
[18]J. L. Martins and N. Troullier (unpublished).
[19]K. Raghavachari and C. M. Rohlfing, J. Chem. Phys. **89**, 2219 (1988).
[20]D. Tomanek and M. Schlüter, Phys. Rev. B **36**, 1208 (1987).
[21]P. Ballone, W. Andreoni, R. Car, and M. Parrinello, Phys. Rev. Lett. **60**, 271 (1988).
[22]K. Raghavachari and J. S. Binkley, J. Chem. Phys. **87**, 2191 (1987); D. Tomanek and M. Schlüter, Phys. Rev. Lett. **67**, 2331 (1991).
[23]J. C. Tully, G. H. Gilmer, and M. Shugard, J. Chem. Phys. **71**, 1630 (1979).
[24]K. S. Pitzer and E. Clementi, J. Am. Chem. Soc. **81**, 4477 (1959).
[25]G. Galli, R. M. Martin, R. Car, and M. Parrinello, Science **250**, 1547 (1990).
[26]C. Z. Wang, C. H. Xu, B. L. Zhang, C. T. Chan, and K. M. Ho, Proceedings of the International Symposium on the Physics and Chemistry of Finite Systems: From Crystals to Clusters, edited by P. Jenna, S. N. Khanna, and B. K. Rao, (Kluwer Academic, Boston/London, in press); and (unpublished).
[27]K. Raghavachari (unpublished).
[28]B. L. Zhang, C. Z. Wang, and K. M. Ho (unpublished).

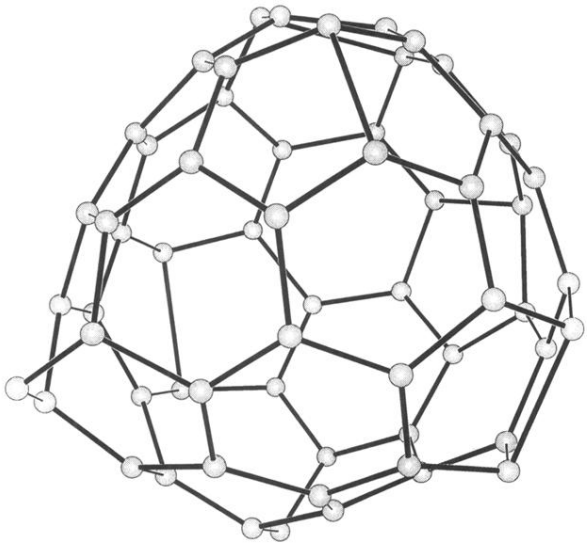

FIG. 6. Lowest energy structure formed from the annealing simulation. Note the presence of both fivefold and sixfold rings. This structure contains elements in common with C_{60}; however, defects still dominate the structure.

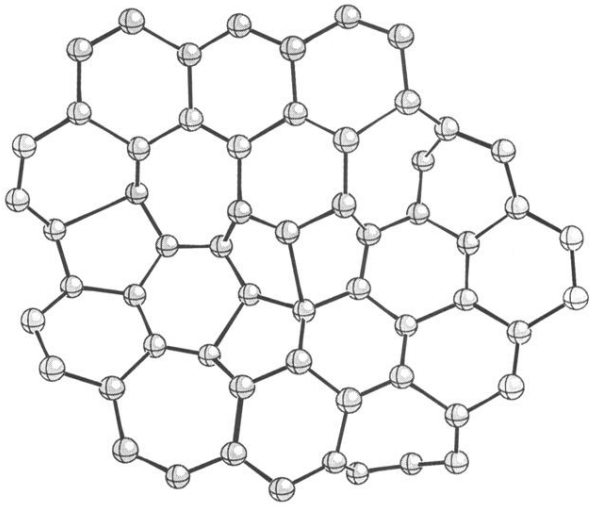

FIG. 7. Structure of carbon atoms quenched within a quasi-two-dimensional constraint. The structure resembles a graphitic sheet with a number of defects introduced by the quick quench.